Supplementary Information: Kovacs-like memory effect in a sheared colloidal glass: role of non-affine flows

Maitri Mandal, Abhishek Ghadai, Rituparno Mandal and Sayantan Majumdar

S1 Estimate of linear response regime in simulation:

As mentioned in the main text, to measure the response under single-step perturbation in the simulation, we monitor the evolution of the stress $\sigma(t)$ just after the application of the perturbation. From this we calculate instantaneous modulus, $\delta\sigma(t)/\delta\gamma = \frac{\sigma(t)-\sigma(0)}{\gamma_1 - \gamma_0}$ and we have plotted the modulus in Fig. S1(a). The evolution of the modulus seem to overlap with each other for a step strain (γ_1) of 0.2% or below; beyond this point, the curves deviate, indicating the onset of nonlinearity.

In Fig. S1(b), we have shown instantaneous modulus for two different step strain γ_1: one in the linear regime ($\gamma_1 = 0.2\%$) and the other beyond the linear regime ($\gamma_1 = 0.5\%$). Similar to what we have observed in experiments, both the curves can be fitted nicely with the same double logarithmic functional form: $\frac{\delta\sigma(t)}{\delta\gamma} = a + b\log(t) + c\log(t+t_0)$ where $a = 0.03989$, $b = -0.01886$, $c = 0.01436$, $t_0 = 17.2831$ for $\gamma_1 = 0.2\%$ and $a = 0.03987$, $b = -0.01977$, $c = 0.01483$, $t_0 = 21$ for $\gamma_1 = 0.5\%$.
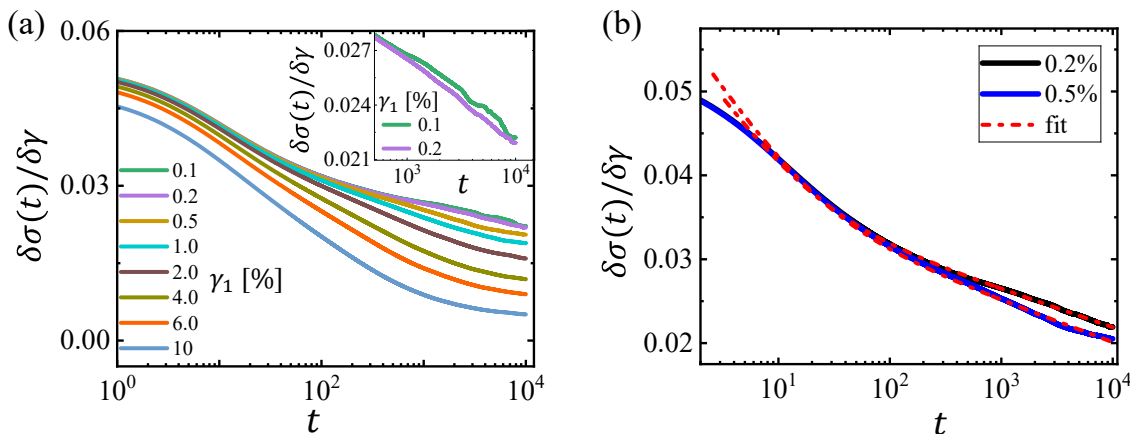
Figure S1: (a) Evolution of the instantaneous modulus $\frac{\delta\sigma(t)}{\delta\gamma}$ for a range of single step perturbation $\gamma_1 = 0.1\% - 10\%$ indicates the linear regime in simulation. In the inset we show the zoomed in version of the relaxation curves (0.1% and 0.2%) at longer time scales. (b) Instantaneous modulus for single-step perturbation is fitted with double logarithmic $\frac{\delta\sigma(t)}{\delta\gamma} = a + b\log(t) + c\log(t+t_0)$ form in both the linear ($\gamma_1 = 0.2$) and non-linear ($\gamma_1 = 0.5$) regime (fitting parameters are described in the text).

S2 Measurement of the peak time deviation:

To measure the deviation of the peak time Δt_{p} from LRT prediction, in both experiments and simulations, we determine the experimental peak time t_p^E and the simulated peak time t_{p}^S from each of the two-step measurements. We have also predicted the peak time t_{p}^P using the linear response theorem in the context of two step strain protocol. Finally we define Δt_{p} as the normalized difference between these two: $\Delta t_{\mathrm{p}} = \frac{|t_{\mathrm{p}}^P - t_{\mathrm{p}}^E|}{t_{\mathrm{p}}^E + t_{\mathrm{p}}^P}$ in experiments, and $\Delta t_{\mathrm{p}} = \frac{|t_{\mathrm{p}}^P - t_{\mathrm{p}}^S|}{t_{\mathrm{p}}^S + t_{\mathrm{p}}^P}$ in the case of simulations.
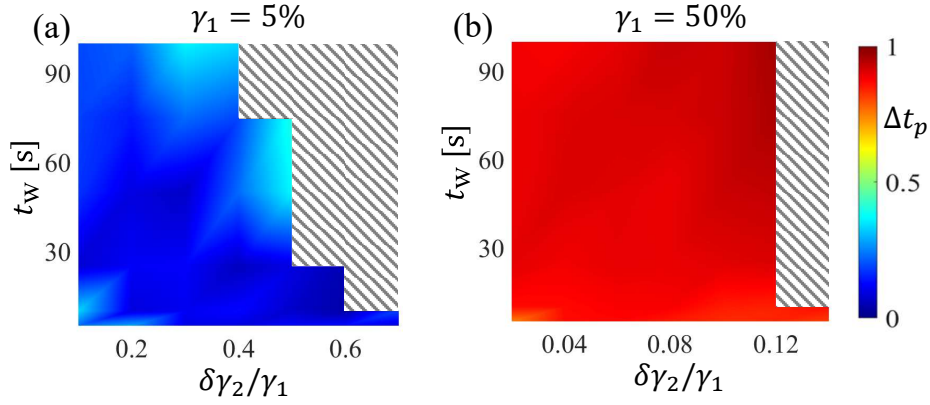
Figure S2: (a) and (b) showing the peak time deviations Δt_{p} for $\gamma_1 = 5\%$ and $\gamma_1 = 50\%$ respectively. The shaded regions where t_{p}^E are absent.

We have shown this quantity Δt_{p} in Fig.3-4 of the main text. Here in Fig. S2(a) and (b) we show the deviation of the peak time (Δt_{p}), measured in experiments, for $\gamma_1 = 5\%$ and $\gamma_1 = 50\%$ respectively. Please note that the $\delta\gamma_2/\gamma_1$ range is not the same for $\gamma_1 = 5\%$ and $\gamma_1 = 50\%$ and we discuss this in detail in the next section.

S3   Absence of peak in the stress response for for larger t_{w} and $\delta\gamma_2$:

As both t_{w} and $\delta\gamma_2/\gamma_1$ increases, the parameter space over which we can reliably obtain the peak, gets smaller. The stress response for large t_{w} and large $\delta\gamma_2/\gamma_1$ gets flatter and it becomes progressively difficult to locate the peak and extract the peak position. This is the reason why the $\delta\gamma_2/\gamma_1$ range is not the same for $\gamma_1 = 5\%$ and $\gamma_1 = 50\%$, as shown in Fig. S2(a) and (b).
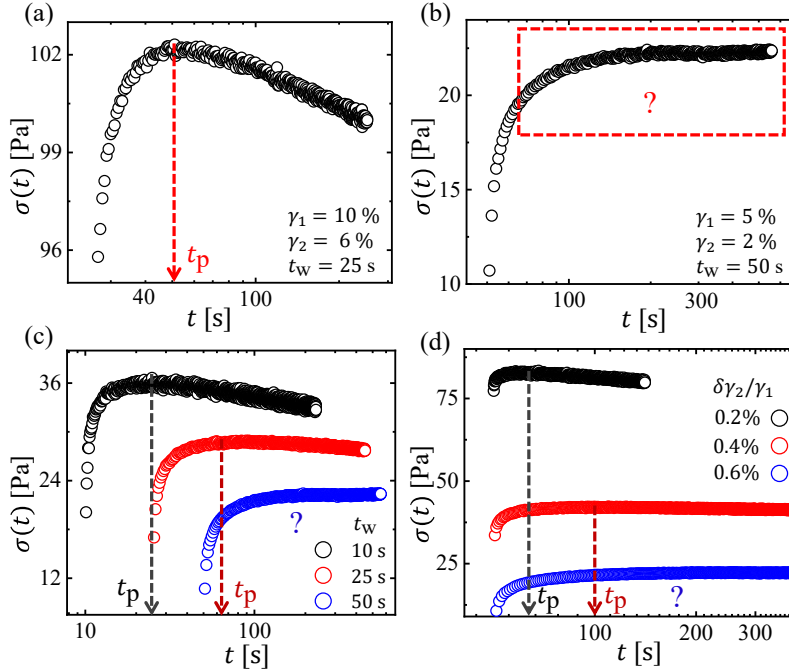
Figure S3: a typical example from experiment where (a) t_{p} is present (b) t_{p} is absent. (c) with increasing t_{w} getting t_{p} becomes harder (data shown for the fixed $\gamma_1 = 5\%$ and $\gamma_2 = 2\%$). (d) For the fixed $\gamma_1 = 5\%$ and t_{w} getting t_{p} of increasing $\delta\gamma_2/\gamma_1$ becomes difficult.

In Fig. S3(a) (for $\gamma_1 = 10\%$, $\gamma_2 = 6\%$ and $t_{\mathrm{w}} = 25s$), we show a typical non-monotonic stress response from the experiment, from which the peak position t_p can be identified very easily whereas, for Fig. S3(b) (for $\gamma_1 = 5\%$, $\gamma_2 = 2\%$ and $t_{\mathrm{w}} = 50s$), there is no clear peak in the stress response. In Fig. S3(c) it has been demonstrated ($\gamma_1 = 5\%$ and $\gamma_2 = 2\%$), that with increasing waiting time t_{w} it becomes harder to identify a clear peak and the corresponding peak time. Similarly in Fig. S3(d) we show, for γ_1 (5%) and t_{w} (50s), the typical stress responses when $\delta\gamma_2/\gamma_1$ increases.

S4 Measurement of the non-affinity in the experiment:

To calculate the non-affinity, we first measure the experimental velocity field $\mathbf{v}^E(x, y)$ and look at the absolute value of the normalised x-component velocity (where x is the shear direction):

$$v^E(x, y) = \left| \frac{v_x^E(x, y)}{v_{max}} \right|$$

where, v_{max} represents the maximum value of the x-component of $\mathbf{v}^E(x, y)$. The experimental velocity field is averaged over different grid points along x-axis at two extremes of the profile, *i.e.* at $y = d$ and $y = 0$, yielding $\langle v^E(d) \rangle_x$ and $\langle v^E(0) \rangle_x$, respectively. Using these mean values, an affine flow field can be computed as:

$$v^A(x, y) = \left[\frac{\langle v^E(d) \rangle_x - \langle v^E(0) \rangle_x}{d} \right] y + \langle v^E(0) \rangle_x.$$

Note that by construction $v^A(x, y)$ depends only on y. Using the experimentally obtained velocity field $v^E(x, y)$ and the corresponding affine velocity field $v^A(x, y)$, we define a measure of non-affinity as:

$$\Delta(x, y) = \frac{\left| v^A(x, y) - v^E(x, y) \right|}{v^A(x, y) + v^E(x, y)}$$

where the denominator acts as a normalization constant. Non-affinity maps $\Delta(x, y)$ for $\gamma_1 = 5\%$ and $\gamma_1 = 50\%$ are shown in Fig. S4.1 (a) and (b) respectively.
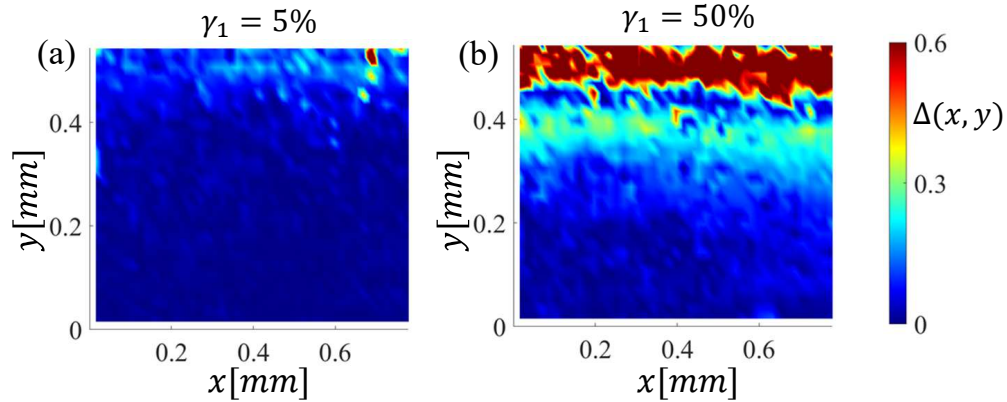
Figure S4.1: The non-affinity map $\Delta(x, y)$ for (a) $\gamma_1 = 5\%$ and (b) $\gamma_1 = 50\%$ respectively, where x is the shear direction and y is the shear gradient direction.
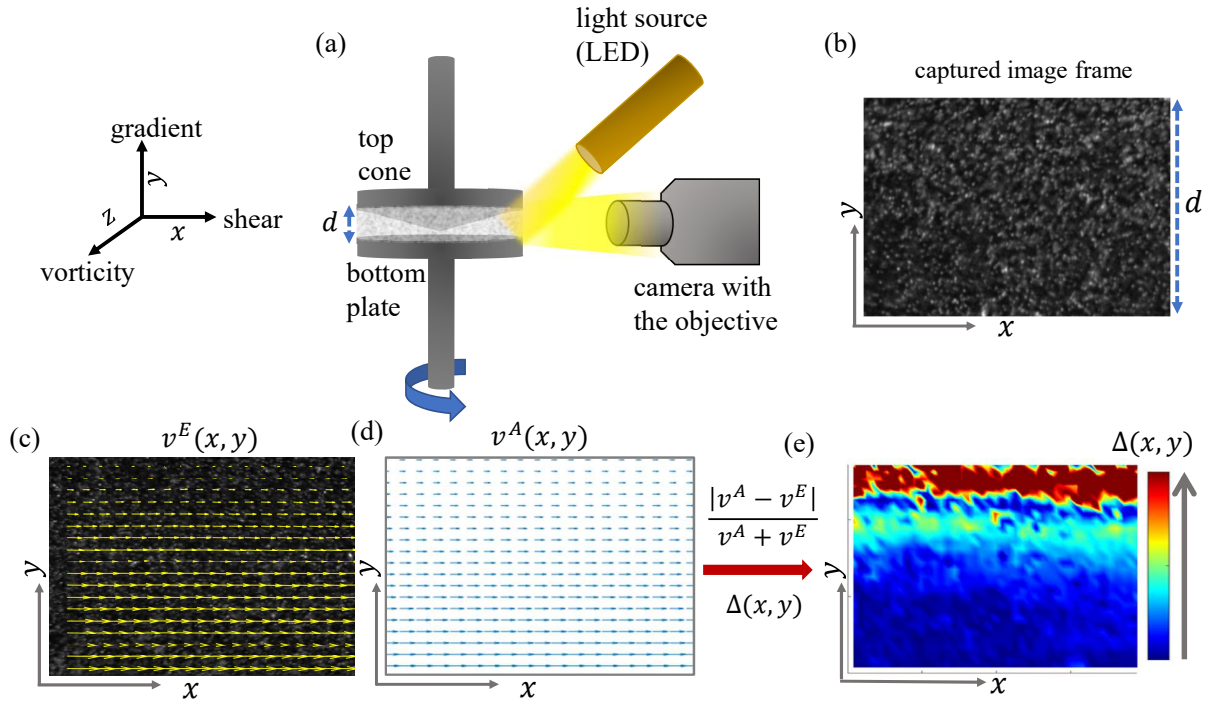
Figure S4.2: The schematic of the imaging setup is shown in Fig.(a), where d represents the width of the sample at the boundary. Fig.(b) presents a typical captured image. By analyzing two such images taken during perturbations and using Particle Image Velocimetry (PIV), we compute the matrix $v^E(x, y)$ which is depicted in Fig.(c). The corresponding affine flow field of the same dimensions, $v^A(x, y)$ is shown in Fig.(d). Finally, Fig. (e) illustrates the non-affinity map $\Delta(x, y)$ obtained by using the $v^E(x, y)$ matrix and the corresponding affine matrix $v^A(x, y)$.

The Fig. S4.2 presents the schematic of the experimental setup along with a pictorial representation of the procedure used to measure the non-affinity map $\Delta(x, y)$.

In our experiments, the size of the grid determines the spatial resolution of velocity mapping. Here, we have chosen the grid size such that each grid is large enough to have a sufficient number of speckles, but significantly small compared to the size of the image to have good enough spatial resolution. In our setup, the size of the tracer particles ($\sim 3.34 \mu m$) and the grid size ($0.02mm \times 0.02mm$) is much larger than the size of the individual PNIPAM particles ($\sim 0.97 \mu m$). Thus, experimentally we cannot probe the particle scale displacements, unlike in simulations.

S5 Dependence of peak height on the waiting time:
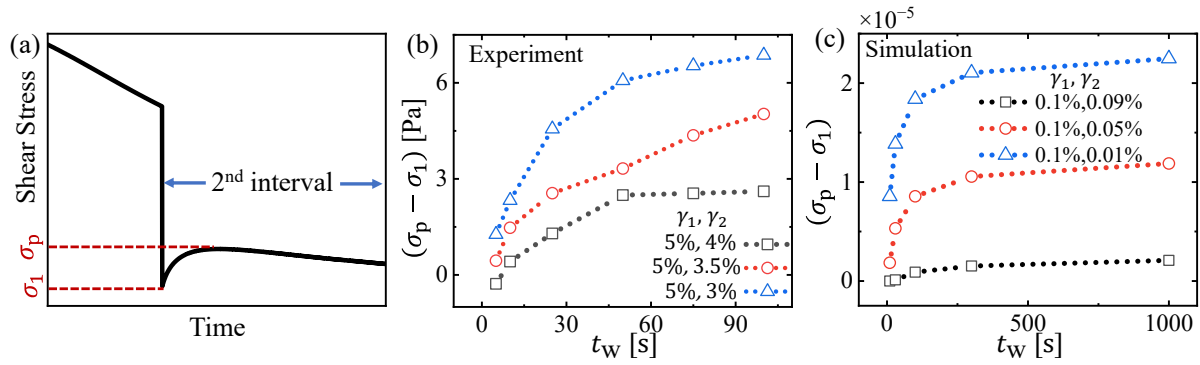
Figure S5: The Fig.(a) shows the cartoon of how we define the peak stress σ_p and the starting stress value σ_1 in the second interval. The Fig.(b) and (c) show the dependence of the peak height with waiting time for (b) $\gamma_1 = 5\%$ in the case of experiment and (c) $\gamma_1 = 0.1\%$ in the case of simulation respectively. Three different plots in each case are for different γ_2 values.

We define the peak height in both cases as $(\sigma_p - \sigma_1)$, where σ_p is the peak stress value in the second interval, and σ_1 is the stress value at the start of the second interval response. In the case of the experiment, σ_1 corresponds to the stress value at $t = t_w + 1$ s, while in the simulation, it corresponds to the stress value at $t = t_w + 0.1$. To examine the dependence of peak height on waiting time, we plot $(\sigma_p - \sigma_1)$ vs. t_w in: Fig. S5 (b) for the experiment ($\gamma_1 = 5\%$, with three different γ_2), and Fig. S5 (c) for the simulation ($\gamma_1 = 0.1\%$, with three different γ_2). In all cases, the peak height initially increases with waiting time and then saturates, consistent with the trend observed in Reference [21] in the main text.

S6 Measurement of the mean deviation of the peak time:

For a given first-step perturbation γ_1, we consider multiple second-step perturbations $\delta\gamma_2 = (\gamma_1 - \gamma_2)$. For each combination of γ_1 and γ_2, a wide range of waiting times is explored in both experiment and simulation. This allows us to calculate the peak time deviation in the second interval relative to the Linear Response Theory (LRT) prediction for all possible parameter combinations. Fig. S6 presents representative examples of these parameter combinations. In the main text, the mean peak time deviation $\bar{\Delta t}_p$ for a given γ_1 accounts for all these parameter regimes.
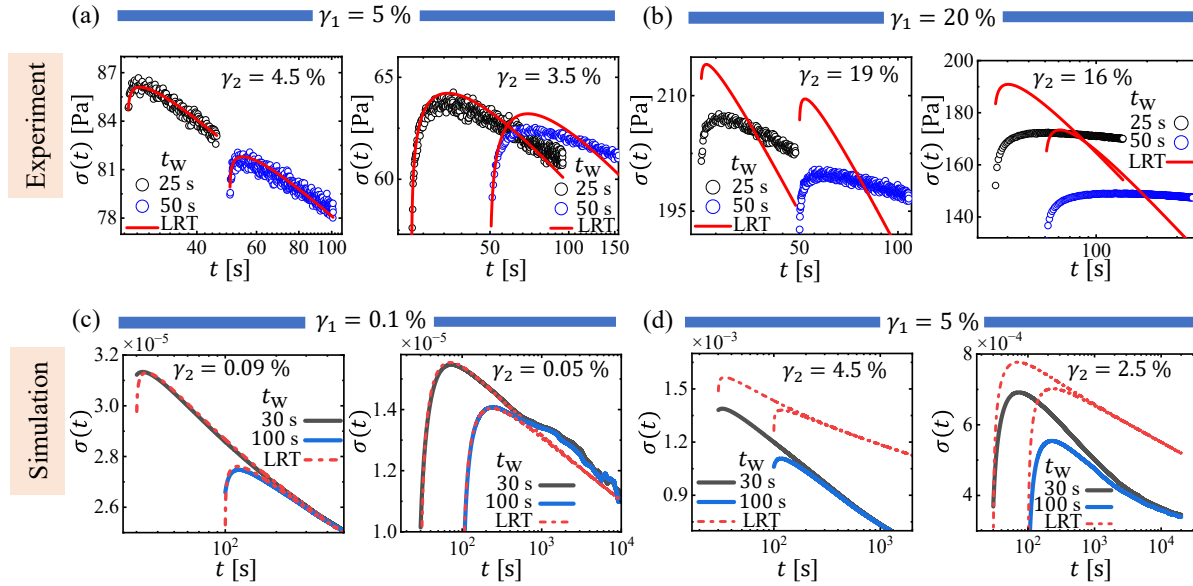
Figure S6: The second interval stress response for various perturbation regimes is compared with the Linear Response Theory (LRT) prediction for both experiment (top panel) and simulation (bottom panel). **Experiment (top panel):** (a) For a smaller perturbation of $\gamma_1 = 5\%$, two secondary strains, $\gamma_2 = 4.5\%$ and $\gamma_2 = 3.5\%$ are selected. (b) For a larger perturbation of $\gamma_1 = 20\%$, two secondary strains, $\gamma_2 = 19\%$ and $\gamma_2 = 16\%$ are chosen. In both cases, stress responses are plotted for two waiting times, $t_w = 25s$ and $t_w = 50s$. Symbols represent experimental data points, while the solid red lines show the LRT predictions. **Simulation (bottom panel):** (c) For a smaller strain of $\gamma_1 = 0.1\%$, two secondary strains, $\gamma_2 = 0.09\%$ and $\gamma_2 = 0.05\%$ are considered. (d) For a larger strain of $\gamma_1 = 5\%$, two secondary strains, $\gamma_2 = 4.5\%$ and $\gamma_2 = 2.5\%$ are chosen. In both cases, stress responses are plotted for two waiting times, $t_w = 30s$ and $t_w = 100s$. Solid lines represent the simulated data, while dashed red lines indicate the LRT predictions.